Direct observation of atomic network migration in glass

You may also be interested in:

Studies of atomic diffusion in Ni–Pt solid solution by x-ray photon correlation spectroscopy
Markus Stana, Michael Leitner, Manuel Ross et al.

Quasi-elastic scattering under short-range order: the linear regime and beyond
Michael Leitner and Gero Vogl

Fast diffusion in a room temperature ionic liquid confined in mesoporous carbon
S. M. Chathoth, E. Mamontov, S. Dai et al.

Atomic caging in multicomponent glass-forming metallic liquids
Kaikin Wong, Changjiu Chen, Michael Marek Koza et al.

The evidence for a metastable phase in norbornadiene: X-ray and quasi-elastic neutron scattering studies
M Bee, J Elkhamkhami and H Jobic

Diffusion studies with synchrotron radiation
Gero Vogl and Markus Hartmann

Ag + dynamics in the superionic and liquid phases of Ag2Se and Ag2Te
M A Hamilton, A C Barnes, W S Howells et al.

Direct observation of atomic network migration in glass

Manuel Ross[1], Markus Stana[1], Michael Leitner[1,2] and Bogdan Sepiol[1]

[1] University of Vienna, Faculty of Physics, Boltzmanngasse 5, 1090 Vienna, Austria
[2] Heinz-Maier-Leibnitz-Zentrum, Technische Universität München, Lichtenbergstraße 1, 85747 Garching, Germany
E-mail: manuel.ross@univie.ac.at

Abstract

Many physical properties of glasses are still far from being understood at the atomic level. The lack of experimental methods capable of studying glassy dynamics at this scale has impeded the development of a complete model for atomic transport processes. Here we apply the new technique of atomic-scale x-ray photon correlation spectroscopy to directly observe single atomic motion in lead silicate glass. We show that dynamics change significantly depending on the glass composition, from single jump processes between inhomogeneous regions to multiple jump processes along network paths and through voids. Up until now, such measurements were far out of reach for temperatures below the glass transition. Our findings suggest that the method and the model introduced here will also help understanding atomic diffusion in a wide range of other glass systems.

Keywords: XPCS, atomic diffusion, lead silicate glass, aXPCS, coherent x-ray scattering, synchrotron radiation

1. Introduction

X-ray photon correlation spectroscopy (XPCS) is a powerful method for studying dynamics in disordered systems. Important groundwork was laid for this field by the pioneering papers of

Sutton *et al* [1] and Brauer *et al* [2]. The most frequent application of XPCS are studies of soft matter dynamics where objects are in the nanometer range (see e.g. 3–7). The capability to resolve single atomic motion in condensed matter with this technique, atomic-scale x-ray photon correlation spectroscopy (aXPCS), has been shown only recently by Leitner *et al* [8]. Moreover, Stana *et al* have shown how to apply this method to less ordered polycrystalline materials [9]. In the metallic glass ZrNiCuAl, the close connection between atomic dynamics and crystallization has demonstrated the failure of the concept of equilibrium diffusion in this material [10]. Recently, Hruszkewycz [11] *et al* have shown that ultrafast dynamics measurements with XPCS on the atomic scale should be feasible. Here we utilize the new method of aXPCS to shed light on the motion at the atomistic level in lead silicate glass below the glass temperature.

Glasses were among the first artificial materials produced by humans, nevertheless their systematic investigation started surprisingly late. The foundations of this research area were laid by Zachariasen [12] and Warren [13]. While the short-range order was rather clear, it was many decades of scientific work later that more detailed models for the intermediate-range order could be provided. This was possible because of the application of many different methods like neutron scattering, extended x-ray absorption fine structure, nuclear magnetic resonance and infrared and Raman spectroscopy [14]. The dynamical behavior of silica glass and other glassy materials is nonetheless still puzzling. The glassy state is normally seen as a dynamically arrested state. Recent findings suggest that even in the deep glassy state in oxide glasses fast atomic rearrangements can happen [15]. Lead silicate glass is of specific interest in structural and dynamical terms, as lead building blocks can cause ion conduction through the glass and as the components lead oxide and silica oxide both can act as network formers, depending on their mixing ratio. While structural details have been revealed recently [16, 17], the principles of the diffusion processes still have to be clarified. Building upon a detailed view of the dynamics, the crucial issue is how these properties are connected to the network-forming role of each component. One of the reasons for these open questions has been the lack of an appropriate method to study glassy dynamics spatially resolved on the atomic scale.

2. Experimental method

2.1. Theory

A good introduction to XPCS can be found in [18 and 19]. The basic idea is that information about the dynamics in real space is stored in a time-series of coherently scattered x-ray intensities. From the autocorrelation function

$$g^{(2)}(\vec{q}, \Delta t) = \left\langle I(\vec{q}, t) I(\vec{q}, t + \Delta t) \right\rangle / \left\langle I(\vec{q}, t) \right\rangle^2, \tag{1}$$

information about the time scale of the underlying atomistic dynamics can be deduced. Here, $I(\vec{q}, t)$ is the observed intensity at scattering vector $\vec{q}$ and at time t and the brackets $\langle ... \rangle$ denote the average over time, i.e. over all pairs of intensity separated by time Δt. Due to the fact that the van Hove pair correlation function can be related to the intensity autocorrelation function [10], the experimentally obtainable values can be linked to the dynamics:

$$g^{(2)}(\vec{q}, \Delta t) = 1 + \beta \exp\left\{ -2\left(\Delta t / \tau(\vec{q})\right)^{\alpha}\right\}. \tag{2}$$

Here the coherence factor [18] β, which can vary between 0 and 1, is a gauge for the degree of coherence. The empirical stretching parameter α can be less than one for a subdiffusive motion of particles [4] or for dynamics where several processes are active. From the obtained correlation time $\tau(\vec{q})$, conclusions on the atomic dynamics can be drawn. The aXPCS technique is a model-dependent technique, like several other methods including Mößbauer spectroscopy [20], time-domain nuclear forward scattering [21] and quasielastic neutron scattering (QENS) [20, 22]. To extract information from the obtained behavior of the correlation time, mathematical models of different diffusion processes are formulated and tested with the experimental $\tau(\vec{q})$ values. In aXPCS the exchange of two atoms of the same species does not affect in any way the scattering pattern, as the configuration of the coherently illuminated volume before and after the jump is indistinguishable. Compared to incoherent methods it is, however, necessary to account for the immediate vicinity of the diffusing species which is usually described by the short-range order parameter. In amorphous materials like lead silicate glasses, the short-range order is still very pronounced, resulting in the so-called structure factor peak. The influence of the surroundings on the movement of each atom has been first described qualitatively for coherent QENS in liquids [23] and is called de Gennes narrowing. The physical principle for this effect is the fact that maxima in the structure factor of liquids and amorphous solids $S_{\mathrm{SRO}}(\vec{q})$ occur at scattering vectors corresponding to the most probable interatomic separation, i.e. they are due to the highly correlated and long-living atomic arrangements. The theory describing the diffuse scattering under short-range order in a linear approximation [24] is discussed in detail by Leitner and Vogl [25]. Calculations within an incoherent scattering theory can be transformed into the form

$$\tau^{-1}(\vec{q}) = \frac{\tau_{\mathrm{inc}}^{-1}(\vec{q})}{S_{\mathrm{SRO}}(\vec{q})}, \tag{3}$$

that can be compared with the results of coherent experiments, where $\tau_{\mathrm{inc}}(\vec{q})$ is the correlation time obtained from incoherent scattering.

2.2. Samples

Two different lead silicate oxide glasses $(PbO)_x(SiO_2)_{1-x}$ have been prepared, with mixing ratios of $x = 30$ mole%, referred to as low lead content glass and $x = 60$ mole%, referred to as high lead content glass. This selection was chosen due to the substantial difference in the structure of lead silicate glasses with these compositions. It has been found that PbO–SiO$_2$ can be classified as a binary network-former glass [17], with emphasis on SiO$_2$ network forming in a low lead content and on PbO network forming in a high lead content silicate glass.

　　Chemically pure materials were used to prepare the glass batches. The finely mixed batches were melted in alumina crucibles in an electrically heated muffle furnace at temperatures ranging between 1123 K for high lead content glass and 1273 K for low lead content glass. The duration of melting was about 1 h and the melts were subsequently quenched to room temperature. The solid specimens were annealed from about 673 K to room temperature with a temperature decrease of about 10 K h^{-1} in order to remove stress. The composition of the samples was analyzed by energy-dispersive x-ray spectroscopy (EDX) showing good agreement with the nominal composition. The glass transition temperature of the samples
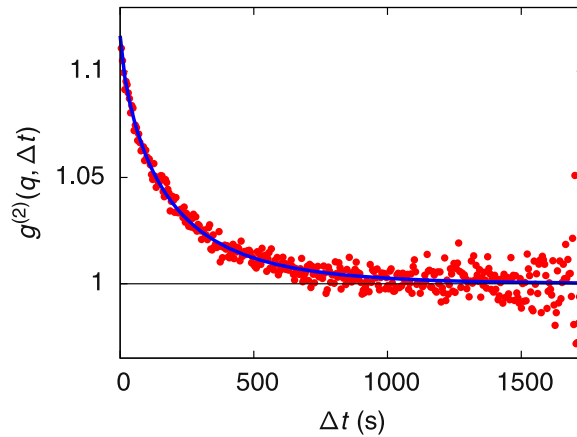
Figure 1. Autocorrelation function $g^{(2)}(q, \Delta t)$ in a high lead content glass sample at $q \approx 0.7\ \text{Å}^{-1}$ and $T = 643$ K. Experimental values were fitted using equation (2) with the parameter $\alpha = 0.75$. The baseline at $g^{(2)} = 1$ is shown for comparison.

was measured by differential scanning calorimetry (DSC) on a NETZSCH DSC 204 Phoenix, yielding values of $T_g \approx 753$ K for low lead content glass and $T_g \approx 663$ K for high lead content glass.

2.3. Setup

The aXPCS experiments were performed at beamline P10 of synchrotron PETRA III using a coherent setup with 7 keV photons for the low lead content and 8 keV photons for the high lead content glass sample. Measurements were performed in a resistively heated vacuum furnace ($p \approx 10^{-6}$ mbar). The temperature was stabilized by a PID controller within a range of 0.1 K at 713 K for low lead content glass and 643 K for high lead content glass. The intensity autocorrelation function was measured for several scattering vectors (see figure 1) and the correlation times were obtained by fitting equation (2) with a free coherence factor β and a stretching parameter $\alpha = 1$ for low lead content and $\alpha = 0.75$ for high lead content glass, respectively. In order to check the stability of the sample as well as the mechanical stability of the setup, the two-time autocorrelation function $C\,(t_1, t_2) = \langle I\,(t_1)I\,(t_2)\rangle/(\langle I\,(t_1)\rangle\langle I\,(t_2)\rangle)$ was calculated for each measurement. For equilibrium systems, the two-time autocorrelation function only depends on $\Delta t = t_2 - t_1$. The few measurements for which instabilities of the setup occurred have been excluded. It should be noted that no significant broadening is observed when evaluating the two-time autocorrelation time. This indicates on the one hand a stable setup and on the other hand the absence of aging in the measured glasses on the atomic scale on the time scale of the measurement. A similar behavior has been found recently by Ruta *et al* [15].

As the detector is not point-like but expands over a span of about 2°, one also averages over a small range of different q-values. For equilibrium systems and with a constant intensity distribution this yields the same result as the pure time average at a sharp q-value, but for significant changes in intensity within the q-range covered by the detector, averaging causes a systematic error. Normally, this error is smaller than the statistical error for our measurements. In high lead content glass, due to the long runtime of our experiment and the changes in scattering intensity with increasing q, the systematic errors get significantly larger than the
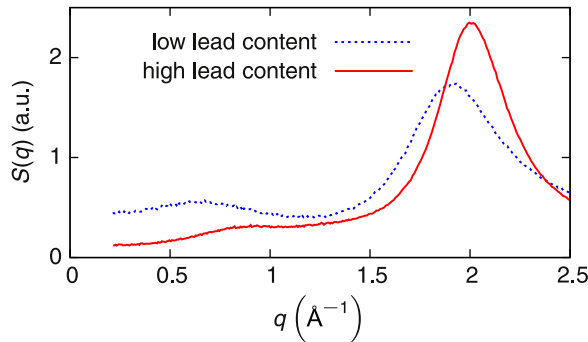
Figure 2. Scattering curves obtained after the experiment for low lead content and high lead content glass.

statistical ones. We have accounted for this systematic error in high lead content glass by virtually splitting the detector area into stripes of equal angular span where the correlation time should not change significantly. The errors given are in that case the difference of the average to the extremal value.

3. Results and discussion

Scattering intensity measurements in a conventional x-ray setup have been performed before and after the XPCS experiments to ensure that no crystallization had occurred. The scattering curves after the experiments are shown in figure 2 for low lead content and high lead content and show no sharp peaks or any other sign of crystallization. The obtained intensities have been used to account for the de Gennes narrowing according to equation (3). We find a first broad peak at about 0.6 Å^{-1} and 0.8 Å^{-1}, respectively. The first broad peak is more distinct in low lead content glass compared to high lead content glass. This was also found in [17], where at low PbO concentrations around 35 mole% there is an inhomogeneous distribution of PbO$_x$ polyhedra resulting in an additional scattering peak at low q-value. At high PbO concentration around 65 mole% the SiO$_4$ structural units are in contrast inhomogeneously distributed. It is of fundamental interest how this change in structure is reflected in the dynamics of the PbO$_x$ building blocks in the network.

Due to the significantly higher scattering cross-section of lead compared to the other elements present in lead silicate glass, we are practically only sensitive to lead atoms and can exclusively follow their dynamics. The dependence of the correlation time on the scattering vector in our aXPCS experiments is shown in figure 3. In low lead content glass, we can utilize a very successful model for jump diffusion derived by Chudley and Elliott [26].

Generally, the resulting inverse incoherent correlation time depends on the normalized jump length distribution $\rho(x)$,

$$\tau_{\text{inc}}^{-1}(q) = \tau_0^{-1}\left(1 - \int_0^\infty j_0(qx)\rho(x)\,\mathrm{d}x\right),\tag{4}$$

where the first spherical Bessel function $j_0(x) = \sin(x)/x$, τ_0 is the mean residence time on one site and $q = |\vec{q}|$. The assumption of Chudley and Elliott was that an atom is trapped in a cage formed by neighboring atoms and, after a certain time, jumps to another site at a fixed distance l in a random direction, which means $\rho(x) = \delta(x - l)$, yielding $\tau_{\text{inc}}^{-1}(q) = \tau_0^{-1}(1 - j_0(ql))$. For
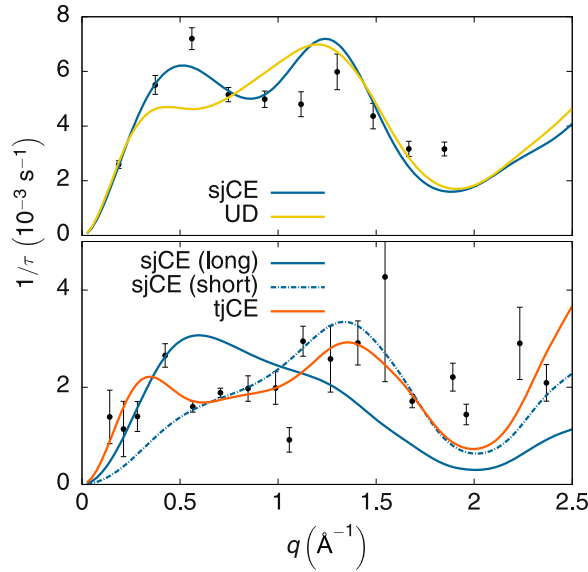
Figure 3. Dependence of the inverse correlation time on the scattering vector for low lead content glass at 713 K (upper plot) and high lead content glass at 643 K (lower plot). The curves show the fit of different models to the data each for low lead content and for high lead content glass (sjCE/tjCE: single jump and two-jump Chudley–Elliott model, UD: model with uniformly distributed jump lengths up to a maximum distance). The long single jump model has been fit only to q-values below 0.5 Å^{-1}, the short single jump model to the whole q-range.

small q-values the sine function can be expanded, resulting in the $|\vec{q}|^{-2}$ divergence of correlation times, which is a very general result valid for liquids as well as for crystalline solids and known as the hydrodynamic limit [22]. For large $|\vec{q}|$ values the correlation time is simply equal to the mean residence time.

Additional models have been applied in comparison to the Chudley–Elliott approach. Those were a Gaussian-like jump length distribution model similar to [27] with a mean jump distance and an additional delocalization parameter of an atom from its site and an extended Chudley–Elliott model, as introduced further below for high lead content glass. Both yield the same fit in the relevant range as the single jump Chudley–Elliott model and are thus not shown in figure 3. Particularly, the two-jump Chudley–Elliott model fit results show that no additional details can be resolved by assuming multiple jump processes for low lead content glass. A further model has been derived for jump lengths which are uniformly distributed ($\rho(x) = 1/l$) for $x \leqslant l$ and 0 otherwise. The resulting inverse correlation time is $\tau_{\text{inc}}^{-1}(q) = \tau_0^{-1}(1 - \text{Si}(ql)/(ql))$, where $\text{Si}(ql)$ is the sine integral and l the maximum jump distance allowed. The fit of this model as shown in figure 3 deviates much stronger from the data than the single jump Chudley–Elliott approach. Concluding the comparison of different models, we find that the single jump Chudley–Elliott model as the most direct approach capturing the details of the experimental data is the most appropriate jump model for low lead content glass. From the medium q-range covered by our experiments, the physical insight about diffusion details on the atomic scale can be obtained. The fit to the data according to the Chudley–Elliott model yields a jump distance of about $l \approx 8(1)$ Å and a mean residence time of $\tau_0 \approx 370$ s. The distances and correlation times measured here are caused by an effective single

jump. From the Einstein relation [28] in the form $D = \langle l^2 \rangle / (6\tau_0)$ we calculate a diffusivity on the order of $10^{-22}\,\mathrm{m^2\,s^{-1}}$. This longer range jump behavior compared to the expected neighboring distance can be attributed to the existence of lead-free regions in the glass. It has been reported for different kinds of glasses [29], that micro-inhomogeneities on the order of $10\,\text{Å}$ in size have been found. This interpretation is also very well reproduced by results obtained in 17. In lead silicate glass of similar composition to our low lead content glass, an aggregation of lead oxide was found, resulting in large amounts of lead-free volume with void sizes of about $15\,\text{Å}$. The stretching parameter $\alpha = 1$ of the fit to our data shows that the jump process has no memory of previous jumps, thus supporting the idea of a single process inside the void structure. A diffusion through these voids has to be fast compared to the mean residence time of a lead atom and the distance should be in the order of the void size, which is in good agreement with our results.

For the high lead content glass, we find that the atomic diffusion undergoes a significant change (figure 3), calling for an extended jump model. Due to the structural inhomogeneity on the short range, different jump processes along locally different jump vector directions are possible. We extend the Chudley–Elliott model to two jump processes to account for this additional feature in the dynamics. This model is based on the same assumptions as the regular Chudley–Elliott model but extended by an additional jump process: $\rho(x) = \omega_1 \delta(x - l_1) + \omega_2 \delta(x - l_2)$. This results in

$$\tau_{\mathrm{inc}}^{-1}(q) = \tau_0^{-1}\Big[1 - \omega_1 j_0(q\,l_1) - (1 - \omega_1)j_0(q\,l_2) \Big], \tag{5}$$

with $\tau_0^{-1} = \tau_1^{-1} + \tau_2^{-1}$ and $\omega_i = \tau_i^{-1}/\tau_0^{-1}$. The factor ω_i is the probability for a jump to have a distance l_i with a mean residence time τ_i.

The measured correlation times are shown together with the model fit in figure 3 and reproduce this extended jump model. The fit yields values of $l_1 \approx 1.2(7)\,\text{Å}$, $l_2 \approx 13(3)\,\text{Å}$, $\omega_1 \approx 0.9$ and $\tau_0 \approx 435\,\mathrm{s}$. From that, we get an overall diffusivity on the order of $10^{-22}\,\mathrm{m^2\,s^{-1}}$ (note the lower temperature compared to the low lead content measurement). Thus about 90% of the atomic jump processes take place on a very short range, while longer range jumps comparable to the situation in the low lead content glass still exist. The stretching parameter $\alpha = 0.75$ of the fit to our data indicates a change in the diffusion process due to the dynamical heterogeneity, which is known to play an important role in the dynamics of glassy materials [30], or in other words the jump process depends on whether a lead atom is placed inside the network structure or at the edge of a void.

As in the case of low lead content glass, additional models have been compared to the extended Chudley–Elliott model in high lead content glass. The Gaussian-like jump length distribution approach and the model of uniformly distributed jump lengths yield the same fit in the relevant range as the single jump Chudley–Elliott approach for short jump distances and are thus not shown in figure 3. As can be seen by comparing the fit of the single jump Chudley–Elliott approach for different q-value ranges to the fit of the extended Chudley–Elliott model, only the latter can capture the details of the data across the whole q-range. In conclusion, we find that the extended Chudley–Elliott approach is the most appropriate jump model for high lead content glass as the most direct approach capturing the details of the experimental data. This demonstrates that a drastic change in dynamics occurs, analogous to the change in structure which has been found for high lead content glasses. In the composition region above
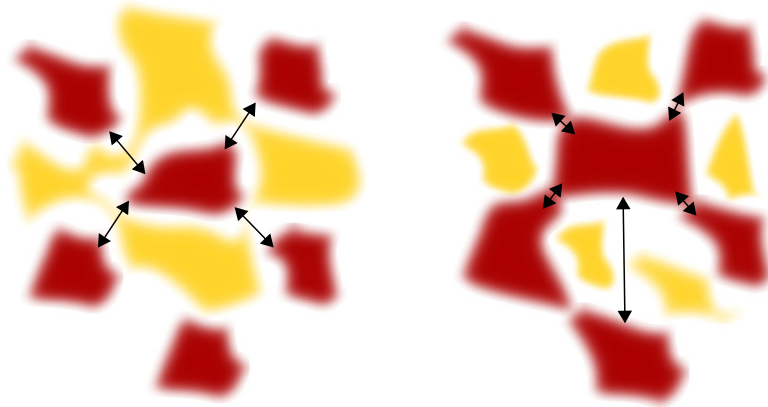
Figure 4. Jump processes of lead oxide in lead silicate glass. Regions in dark (red) color represent regions of lead oxide aggregation, regions in light (yellow) color represent silica oxide structures. Left: for low lead content glass, the diffusive motion is driven by jumps between regions of lead oxide aggregation. Right: in high lead content glass, two distinct types of jump processes exist. The network connectivity allows for a short-range diffusion along network paths, also jump processes through the voids over longer distances contribute to the diffusion.

50 mole% PbO, lead oxide forms the network while the silica oxide building blocks get mostly isolated [17].

The increased jump distance for the longer range jumps in high lead content glass compared to the motion in low lead content glass can be attributed to the tendency for larger voids in the structure, enabling a longer-range mobility of the PbO building blocks. This concurs well with the most surprising result in the study of Kohara *et al* [17] claiming that in contrast to the common opinion lead silicate glasses contain extraordinarily large amounts of free volume or voids. Recent studies of Kaur *et al* [31] support this view showing that lead silicate glasses do not exhibit an abrupt increase in volume at the glass transition temperature which would occur in a densely packed system.

4. Conclusion

Combining our results for the different lead compositions, we find that a split of the dynamics occurs. Longer range single jump processes dominate the motion in low lead content glass whereas at least two different jump processes, one on the short range and at least one other on the long range, dominate the motion in high lead content glass. With these findings, lead diffusion can be understood as a consequence of direct jumps between regions of PbO aggregation in low lead content glass and as a consequence of short range motion between connected regions of lead oxide aggregation and longer range direct jumps through voids in high lead content glass. The clear transition in atomic motion from a single jump process in low lead content to a two-jump process in high lead content glass indicates a change in the dynamics hand in hand with the change in structure. The existence of jump processes on distinctly different length scales can be attributed to two structural features. First, the longer range jumps imply a still existing partial aggregation of lead in high lead content silicate glass and resulting voids between these aggregations. Secondly, the much more frequent short range jumps show

that by the percolation of the PbO network structure, diffusion is possible along the strongly connected regions of PbO aggregation (see figure 4).

In this study we utilized the aXPCS technique for lead silicate glasses to obtain detailed insight into atomic transport, revealing the characteristic jump distances and the connection between the structural heterogeneity of different glass compositions and the change in the diffusion processes. These findings lead to the conclusion that even at this general level, a consistent description of transport properties in lead silicate glasses can be achieved. Studying further glass systems with aXPCS in a similar fashion promises to yield deeper insight and enhance the understanding of atomic diffusion in amorphous systems.

Acknowledgments

References

[1] Sutton M, Mochrie S G J, Greytak T, Nagler S E, Berman L E, Held G A and Stephenson G B 1991 Observation of speckle by diffraction with coherent x-rays *Nature* **352** 608–10

[2] Brauer S, Stephenson G B, Sutton M, Brüning R, Dufresne E, Mochrie S G J, Grübel G, Als-Nielsen J and Abernathy D L 1995 X-Ray intensity fluctuation spectroscopy observations of critical dynamics in Fe₃Al *Phys. Rev. Lett.* **74** 2010–3

[3] Grübel G, Madsen A and Robert A 2008 X-Ray photon correlation spectroscopy (XPCS) *Soft-Matter Characterization* ed R Borsali and R Pecora (Berlin: Springer) pp 935–95

[4] Guo H, Bourret G, Lennox R B, Sutton M, Harden J L and Leheny R L 2012 Entanglement-controlled subdiffusion of nanoparticles within concentrated polymer solutions *Phys. Rev. Lett.* **109** 055901

[5] Cipelletti L and Weeks E R 2011 Glassy dynamics and dynamical heterogeneity in colloids *Dynamical Heterogeneities in Glasses, Colloids and Granular Media* ed L Berthier, G Biroli, J-P Bouchaud, L Cipelletti and W van Saarlos (Oxford: Oxford University Press) pp 110–51

[6] Chushkin Y, Caronna C and Madsen A 2012 A novel event correlation scheme for x-ray photon correlation spectroscopy *J. Appl. Crystallogr.* **45** 807–13

[7] Robert A, Wagner J, Autenrieth T, Härtl W and Grübel G 2005 Structure and dynamics of electrostatically interacting magnetic nanoparticles in suspension *J. Chem. Phys.* **122** 084701

[8] Leitner M, Sepiol B, Stadler L-M, Pfau B and Vogl G 2009 Atomic diffusion studied with coherent x-rays *Nat. Mater.* **8** 717–20

[9] Stana M, Leitner M, Ross M and Sepiol B 2013 Studies of atomic diffusion in Ni–Pt solid solution by x-ray photon correlation spectroscopy *J. Phys.: Condens. Matter* **25** 065401

[10] Leitner M, Sepiol B, Stadler L-M and Pfau B 2012 Time-resolved study of the crystallization dynamics in a metallic glass *Phys. Rev.* B **86** 064202

[11] Hruszkewycz S O *et al* 2012 High contrast x-ray speckle from atomic-scale order in liquids and glasses *Phys. Rev. Lett.* **109** 185502

[12] Zachariasen W H 1932 The atomic arrangement in glass *J. Am. Chem. Soc.* **54** 3841–51

[13] Warren B 1934 The diffraction of x-rays in glass *Phys. Rev.* **45** 657–61

[14] Rao K J 2002 *Structural Chemistry of Glasses* (Amsterdam: Elsevier)

[15] Ruta B, Baldi G, Chushkin Y, Rufflé B, Cristofolini L, Fontana A, Zanatta M and Nazzani F 2014 Revealing the fast atomic motion of network glasses *Nat. Commun.* **5**

[16] Takaishi T, Takahashi M, Jin J, Uchino T, Yoko T and Takahashi M 2005 Structural study on PbO–SiO$_2$ glasses by x-ray and neutron diffraction and ^{29}Si MAS NMR measurements *J. Am. Ceram. Soc.* **88** 1591–6

[17] Kohara S, Ohno H, Takata M, Usuki T, Morita H, Suzuya K, Akola J and Pusztai L 2010 Lead silicate glasses: binary network-former glasses with large amounts of free volume *Phys. Rev.* B **82** 134209

[18] Sutton M 2008 A review of x-ray intensity fluctuation spectroscopy *C. R. Phys.* **9** 657–67

[19] Abernathy D, Grübel G, Brauer S, McNulty I, Stephenson G, Mochrie S, Sandy A, Mulders N and Sutton M 1998 Small-angle x-ray scattering using coherent undulator radiation at the ESRF *J. Synchrotron Radiat.* **5** 37–47

[20] Vogl G and Sepiol B 2005 The elementary diffusion step in metals studied by the interference of gamma-rays, x-rays and neutrons *Diffusion in Condensed Matter* ed P Heitjans and J Kärger (Berlin: Springer) pp 65–91

[21] Sepiol B, Meyer A, Vogl G, Rüffer R, Chumakov A I and Baron A Q R 1996 Time domain study of Fe-57 diffusion using nuclear forward scattering of synchrotron radiation *Phys. Rev. Lett.* **76** 3220–3

[22] Hempelmann R 2000 *Quasielastic Neutron Scattering and Solid State Diffusion* (Oxford: Oxford University Press)

[23] de Gennes P 1959 Liquid dynamics and inelastic scattering of neutrons *Physica* **25** 825–39

[24] Sinha S and Ross D 1988 Self-consistent density response function method for dynamics of light interstitials in crystals *Physica* B **149** 51–56

[25] Leitner M and Vogl G 2011 Quasi-elastic scattering under short-range order: the linear regime and beyond *J. Phys.: Condens. Matter* **23** 254206

[26] Chudley C T and Elliott R J 1961 Neutron scattering from a liquid on a jump diffusion model *Proc. Phys. Soc. London* **77** 353–61

[27] Jobic H and Theodorou D N 2007 Quasi-elastic neutron scattering and molecular dynamics simulation as complementary techniques for studying diffusion in zeolites *Microporous Mesoporous Mater.* **102** 21–50

[28] Einstein A 1905 Über die von der molekularkinetischen Theorie der Wärme geforderte Bewegung von in ruhenden Flüssigkeiten suspendierten Teilchen *Ann. Phys.* **322** 549–60

[29] Bus'ko I, Golubkov V and Stolyarova V 2003 On the structure of low-alkali rubidium and cesium borate glasses and melts *Glass Phys. Chem.* **29** 267–75

[30] Chaudhuri P, Berthier L and Kob W 2007 Universal nature of particle displacements close to glass and jamming transitions *Phys. Rev. Lett.* **99** 060604

[31] Kaur A, Khanna A, Singla S, Dixit A, Kothiyal G P, Krishnan K, Aggarwal S K, Sathe V, Gonzalez F and Gonzalez-Barriuso M 2013 Structure-property correlations in lead silicate glasses and crystalline phases *Phase Transit.* **86** 759–77